Near edge x-ray absorption spectroscopy: a novel approach for determining conduction band edge states in transition metal oxide gate dielectrics

2005 Phys. Scr. 2005 335

(http://iopscience.iop.org/1402-4896/2005/T115/093)

Physica Scripta. Vol. T115, 335–338, 2005

Near Edge X-Ray Absorption Spectroscopy: a Novel Approach for Determining Conduction Band Edge States in Transition Metal Oxide Gate Dielectrics

G. Lucovsky[1,*], Y. Zhang[1], J. L. Whitten[2], D. G. Schlom[3] and J. L. Freeouf[4]

[1]Department of Physics, North Carolina State University, Raleigh, NC 27695-8202, USA
[2]Department of Chemistry, North Carolina State University, Raleigh, NC 27695, USA
[3]Department of Materials Science, Pennsylvania State University, College Park, PA 16802, USA
[4]Department of Electrical Engineering, Oregon Graduate Institute, Portland, OR 97291, USA

Received June 26, 2003; accepted October 22, 2003

PACS numbers: 71.15.Nc, 71.15.Qe, 78.20.−e, 78.40.−q, 78.70.Dm

Abstract

Spectroscopic studies of transition metal (Tm) and rare earth (Re) oxides, combined with *ab initio* theory identify the band edge electronic structure of alternative high-K dielectrics. The lowest conduction band states are derived from anti-bonding transition metal d*-states with a π symmetry and show strong final state effects. Applied to the complex Tm/Re mixed oxides of the general form $ReTmO_3$, this approach identifies a novel way for obtaining separate and independent control of band gap energies and dielectric constants through local bonding arrangements in which Tm and Re atoms are nearest neighbors to the same oxygen atom.

1. Introduction

The band edge electronic structure of the group IVB Tm oxides, TiO_2, ZrO_2, and HfO_2, has been obtained by X-ray absorption spectroscopy (XAS) and vacuum ultra-violet spectroscopic ellipsometry (VUV SE), coupled with *ab initio* calculations and provides the basis for a quantitative understanding of empirically-determined scaling of band gaps and band offset energies with respect to Si as function of the atomic d-state energies of the respective Tm/Re atoms. Based on this scaling, and confirmed by experiment, elemental oxides, and silicate and aluminate alloys containing Sc, Ti, Ta and Nb have band offset energies too small for reducing direct tunneling to levels required for advanced devices in spite of high dielectric constants and film thickness increases of 5 to 10 relative to SiO_2.

Spectroscopic studies of $GdScO_3$ provide an additional dimension to this scaling. Based on XAS and VUV SE measurements, and combined with an extension of *ab initio* calculations to complex oxides with Re-O-Tm bonding arrangements, it is shown that coupling of Re and Tm atomic d-states in these arrangements increases minimum band gaps and conduction band offset energies with respect to crystalline Si, thereby identifying novel and technologically important opportunities for band gap 'engineering' at the atomic scale.

2. Spectroscopic studies of group IVB Tm oxides and $GdScO_3$

The lowest conduction band states of ZrO_2 as determined from Zr $M_{2,3}$ and O K_1 XAS [1], and band edge optical absorption constants from VUV SE measurements [2] are associated with symmetry-split Zr 4d*-states, and a broader band derived form Zr5s*-states. Table I summarizes the relative energies of these spectral features for ZrO_2, as well as HfO_2 and TiO_2. Relative energies of these features in the $X_{2,3}$ spectra (X = L, M and N) normalized to the lowest d*-state energy, are essentially the same for ZrO_2 and HfO_2, except for a small difference in the d*-s* state splitting. In contrast, the d* state splitting in the TiO_2 $L_{2,3}$ spectra is smaller, and the d*-s* splitting is larger. Due to final state effects the d* state splitting show differences in the respective Tm $X_{2,3}$, O K_1 and absorption edge spectra. Figure 1 displays corresponding spectra for $GdScO_3$: the $L_{2,3}$ spectrum for Sc in Fig. 1(a), the O K_1 edge spectrum in Fig. 1(b), the optical absorption constant in Fig. 1(c), and additional absorption edge transmission for intra 4f-level transitions in Fig. 1(d) [3].

Table I. *Measured d*-d* and d*-s* splittings.*

oxide	$X_{2,3}$ d*-d* (d*-s*) ±0.2 eV	K_1 edge d*-d* (d-s) ±0.2 eV	band edge d*-d* (d*-s*) ±0.2 eV
TiO_2	2.0 (13)	1.8 (6)	1.4 (5)
ZrO_2	2.4 (12)	1.3 (4.5)	∼1.4 (<1)
HfO_2	∼2 (10)	1.5 (4.5)	∼1.4 (<1)

The features in the $L_{2,3}$ spectrum in Fig. 1(a) are associated with localized transitions between spin-orbit split Sc $2p_{1/2}$ and $2p_{3/2}$ states and symmetry split Sc 3d* states. Matrix element effects account for the lack of observable absorption from the Sc states to anti-bonding Sc 4s* states [4]. The spin-orbit splitting is ∼4 eV, the symmetry splitting of the 3d*-states is ∼2 eV, and the spectral width is <0.5 eV (the spectral resolution is ∼0.2 eV).

The two features at ∼532.5 and 536 eV in the O K_1 edge in Fig. 1(b) are associated with transitions to d*-states. Based on relative widths, the lower energy feature is Sc 3d*-like, and the higher is Gd 5d*-like. The splitting between these states, ∼3.5 eV is smaller than the splitting of ∼4.2 eV in ZrO_2 (4d*) and HfO_2(5d*), but larger than the 2.5 eV splitting in TiO_2 (3d*).

Figure 1(c) displays the optical absorption constant, α, at the band edge as a function of photon energy obtained from the analysis of VUV SE data. The transmission measurement in Fig. 1(d) establishes that the features between about 4.8 and 5.8 eV are due to intra 4f-level transitions characteristic of the partially occupied 4f-shell in Gd [5]. The rapid rise of absorption at approximately 5.8 eV in Fig. 1(c) marks the onset of transitions from the top of valence band, O 2p π non-bonding states, to the lower of the two d*-states. Since there is no distinct

*e-mail: lucovsky@unity.ncsu.edu

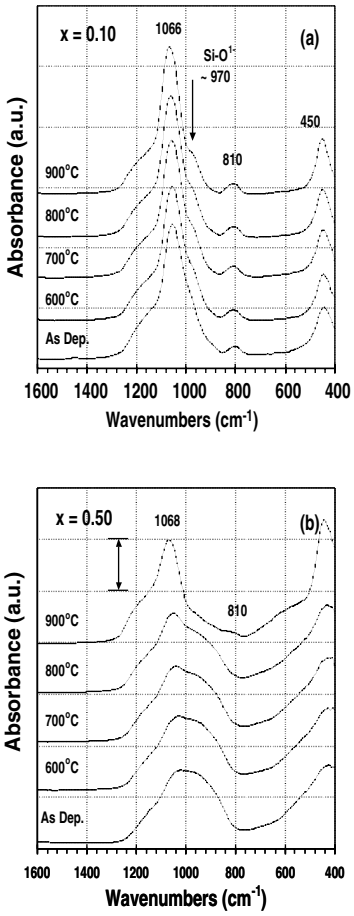

Fig. 1. $GdScO_3$ spectra: (a) $L_{2,3}$ spectrum for Sc, (b) O K_1 edge spectrum, (c) band edge absorption constant, and (d) transmission.

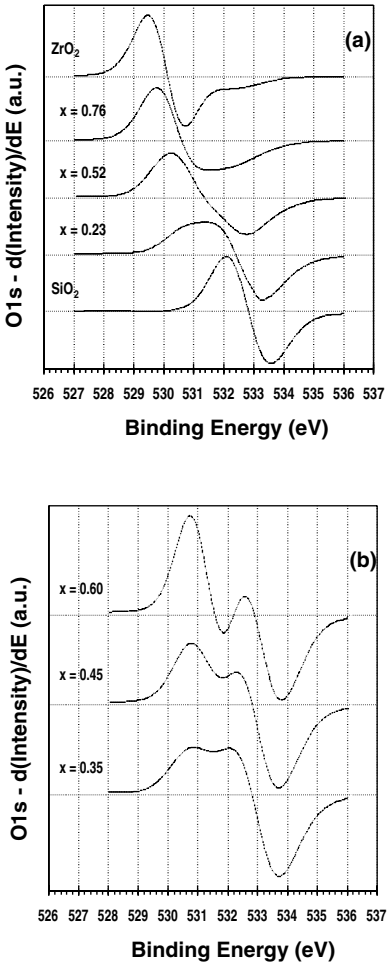

Fig. 2. Calculated band edge electronic structure of ZrO_2 and TiO_2. Energies are referenced to the top of the valence band.

spectral evident for the second d*-state, absorption above 6 eV is dominated by transitions to s*-states.

3. *Ab initio* calculations

The spectra for the group IVB oxides have been interpreted through *ab initio* calculations, the details of which will be published elsewhere [6]. The electronic structure calculations employ variational methods in which an exact Hamiltonian is used so that the variation principle applies. The calculations are done initially through a self-consistent field (SCF) Hartree-Fock calculation with a single determinant wave function, which does not include electron correlation. Following this, there is a configuration interaction (CI) refinement of the bonding orbitals based on a multi-determinant expansion wave function, and including electron correlation effects.

This method has been applied to small clusters that include the bonding of the transition metal atom to O neighbors terminated by H atoms. Calculations have been made for the ground state energy, and the Zr K_1, the Zr $M_{2,3}$, the O K_1, and the absorption edge transitions and the corresponding electronic structures for TiO_2, and HfO_2. Table I summarizes the relative energies of these spectral features for ZrO_2, as well as HfO_2 and TiO_2. Relative energies of these features in the $X_{2,3}$ spectra (X = L, M and N) normalized to the lowest d* state energy, are essentially the same for ZrO_2, HfO_2, and TiO_2 except for small differences in the d*-s* state splitting. The d*-d*, and d*-s* splittings are smaller in the K_1 edge and band edge spectra as well. The d*-s* splitting are greater for TiO_2, with no d*-s* overlap in the band edge spectra, as contrasted with marked overlap for both ZrO_2 and HfO_2. This trends have been are in agreement with theory.

Figure 2 compares the calculated band edge structures of ZrO_2 and TiO_2. All energies are referenced to the top of the valence band, which is comprised of oxygen atom 2p π non-bonding states. Consider first the valence band states. In order of increasing binding energy these are non-bonding O 2p π, and 3d Ti or 4d Zr π-bonded states, and 3d Ti or 4d Zr σ-bonded states with the corresponding O 2p π or σ orbitals. The overlap is larger for the Ti 3d-O 2p π-bonding than for Zr 4d-O 2p π-bonding, hence the difference of $\sim$2 eV. The differences in relative energy between the Ti 3d-O 2p and Zr 4d-O 2p σ-bonding states are similar as indicated by the dashed arrows. The separation of the conduction band d-states comes from the calculations, and the relative energy of the lowest conduction band state is from experiment. The energies of the lowest Tm conduction band states have a reversed π^*/σ^* ordering, and the energies relative the atomic Ti 3d and Zr 4d states and are respectively smaller consistent with the *bonding stabilization energy* being greater than the *anti-bonding destabilization energy*.

One of the more important features of Fig. 2 is the energy difference between the respective atomic d-states, 11.1 eV for the Ti 3d state, and 8.13 for the Zr 4d state, and the respective lowest anti-bonding states. This is approximately 2 eV, and is the basis for the scaling of elemental oxide band gaps with the energies of the respective atomic d-states that is displayed in Fig. 3. This explains the approximately linear dependence in the energy range between

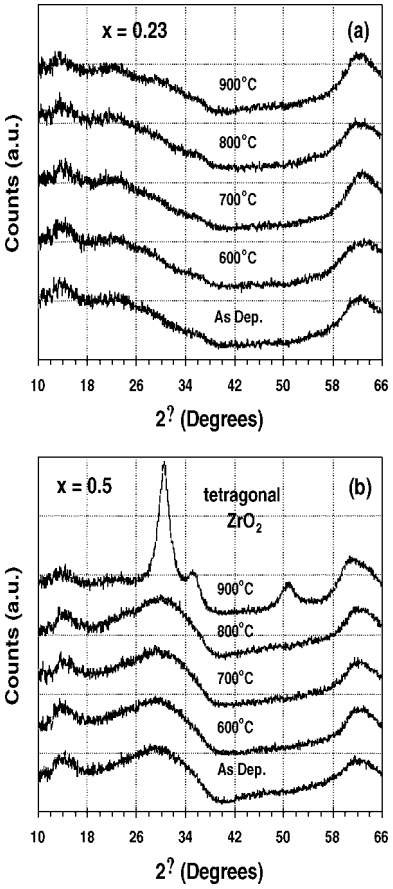

Fig. 3. (a) Empirical scaling of band gaps versus atomic d-state energy. Solid line – trend for transition metal oxides, dashed line – predicted scaling for complex oxides with d-state coupling. 3(b) Empirical scaling of conduction band offset energies with respect to Si versus atomic d-state energy. Solid line – trend for transition metal oxides, dashed line – predicted scaling for complex oxides with d-state coupling.

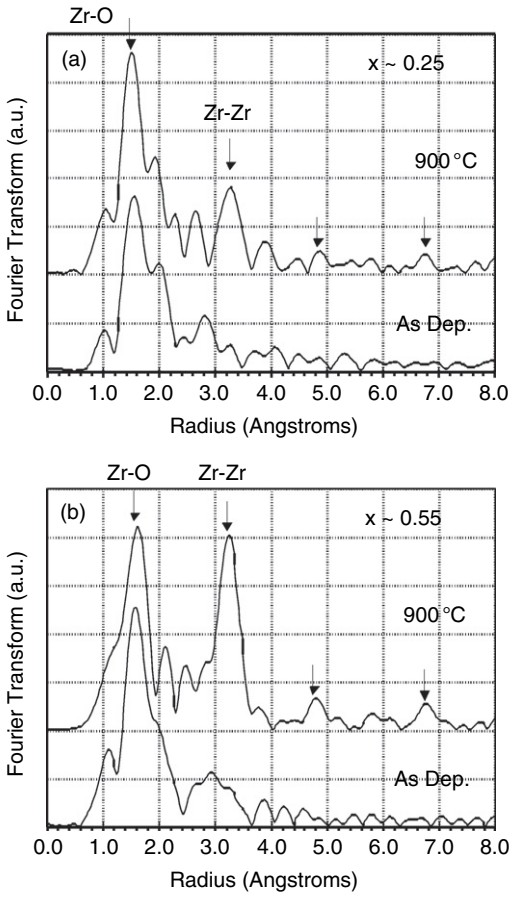

Fig. 4. Schematic representation of molecular orbitals for band edge electronic structure. Top: for elemental transition metal and rare earth oxides; bottom; for complex oxides with d-state coupling through O-atoms.

-11 and -8 eV, which includes in order of increasing (more positive) d-state energy, Ti, Nb, Ta, Sc, Zr and Hf. The bending over at higher energies, e.g., for Y or La, is a manifestation of interactions between higher lying $(n + 1)$ s*-states, and the n d*-σ–state band. The flattening out at lower energy occurs for oxides of Mo and W (not high-K candidates) where d-state occupancy is increased.

Based on this scaling, and results presented in Ref. [7], the minimum band gap in $GdScO_3$ is expected to be determined by transitions which terminate in d*-states with Sc 3d*-character. Since the top of the valence is O 2p p non-bonding, the valence band relative to vacuum are expected to be essentially the same in Sc_2O_3 and $GdScO_3$. The band gap for Sc_2O_3 as determined from transitions terminating in the lowest lying 3d*-state is a approximately 4.3 ± 0.1 eV [7], scaling arguments would place the lowest band gap in $GdScO_3$ at approximately the same energy, and less than 4.5 eV. This expectation is based on comparisons between the band gaps of TiO_2 and $SrTiO_3$, and Nb_2O_5 and $KNbO_3$ [8], where the respective band gaps differ by no more than 0.2 eV.

4. Interpretation of the spectra for $GdScO_3$

Since the lowest band gap in $GdScO_3$ is at ~4.9 eV, this represents a marked departure from the scaling discussed above. This is accounted for by considering differences between the bonding in $GdScO_3$ and the elemental oxides and oxides in Fig. 4. The local bonding in $GdScO_3$ includes arrangements in which both Gd and Sc atoms are bonded to the same O atom. This promotes a mixing of Sc 3d-states and Gd 5d-states, which contributes to both the valence band and conduction band electronic structure. Figure 4 presents an energy band scheme that applies. The upper part of the figure illustrates bonding in elemental Tm or Re oxides, e.g., Sc_2O_3 or Gd_2O_3, in which Tm or Re atoms, respectively, are second neighbors and bonded to a common O atom. The lower portion indicates changes that occur in complex oxides in which Tm and Re atoms are second neighbors through bonding to the same O atom. For $GdScO_3$, the overlap of the Sc 3d states both for π- and σ-bonding is greater than for the Gd 5d states, and this results in valence band, and anti-bonding states that are shifted in energy from their respective end member oxides, Sc_2O_3 and Gd_2O_3. Based on overlap integral differences, valence band π- and σ-states are at intermediate energies with respect to the corresponding elemental oxides states. This increases the energy of the lowest conduction band state with respect to Sc_2O_3, and also makes the separation between the two d*-states intermediate between those of a 3d-oxide and 5d-oxide. This is important for band gap/band offset energy scaling, and is included in Fig. 3.

The basis for the scaling comes from comparisons between $GdScO_3$ and ZrO_2, where the onsets of strong absorption occur respectively at 5.8 and 5.7 eV; this means that $GdScO_3$ has a band gap characteristic of a 4d Tm oxide. It is interesting to note that the average atomic d-state energy in $GdScO_3$, equal 0.5 $(-6.6\,\text{eV} + -9.4\,\text{eV}) = -8\,\text{eV}$ which approximately equal the atomic d-state energy of ZrO_2, -8.13 eV. In a parallel manner, the band gaps of ScO_3, ~4.5 eV and Gd_2O_3, ~6.3 eV average out

to a band gap of approximately 5.5 eV. This suggests that a virtual crystal model can be applied to complex Tm/Re oxides in which d-states of the constituent atoms are coupled through bonding to common O atoms. Bonding in Tm/Re silicates and aluminates is qualitatively different and has been addressed in Ref. [1] and [9]. The energies of Zr core states, and Si core states track across Zr silicate alloys with a constant separation [9]. This equivalent to the difference between the band edge transitions between O 2p π non-bonding states and Zr 4d* and Si 3s* states maintaining a constant energy separation that is shown in Ref. [1]. Tm (Re) silicate and aluminate alloys are the *two band* systems, where energies are maintained at relative end-member oxide levels, but relative absorptions change with relative concentration, whilst the complex $ReTmO_3$ display a qualitatively different *single band* behavior. Oxides with Gd_2O_3 and Sc_2O_3, with other than the 1 : 1 ratio are expected to display spectra characteristic of more than one environment; e.e., Sc_2O_3 rich alloys, should display multiple d*-state features at energies characteristic of both Sc-O-Sc, and Sc-O-Gd bonding arrangements.

5. Discussion

Figure 4 includes the application of the virtual crystal model to complex oxides. The square point is the experimental value for $GdScO_3$ and is plotted at the Sc atomic d-state energy of 9.35 eV. The diamond shape point is for a HfO_2 (5d) – Tio_2 (3d), 1 : 1 alloy, $TiHfO_4$, where the band gap is the average of HfO_2 (5.8 eV) and TiO_2 (3.1 eV) or 4.4 eV. The conduction band offset energies are estimated on the basis of the virtual crystal model. $GdScO_3$ is 'equivalent' to ZrO_2 with an offset of 1.5 eV, and $Hf(Zr)TiO_2$ is expected to have an offset energy of approximately 1 eV, whereas a Ta_2O_5-$2HfO_2$ alloy may have an offset as high as 1.4 eV. Thin film alloys are being prepared to test these predictions of the virtual crystal model. If they prove to be correct, then a virtual crystal behavior should occur in the dielectric constants as well, and therefore provide separate and independent control of offset energies and K. This would be particularly interesting for the TiO_2 and Ta_2O_5 complex oxides where the dielectric constants of the elemental Tm oxides, $\sim$50, and 30, respectively.

Acknowledgements

Supported by the SRC, ONR and NSF.

References

1. Lucovsky, G. *et al*., J. Vac. Soc. Technol. **B 20**, 1739 (2002).
2. Lim, S.-G. *et al*., Appl. Phys. **91**, 4500 (2002).
3. Haeni, J. H. *et al*., J. Appl. Phys. (2003), in process.
4. Condon, E. U. and Shortley, G. H., "Theory of Atomic Spectra" (Cambridge, London, 1935).
5. McClure, D. S., "Electroic Spectra of Molecules and Ions in Crystals" (Academic Press, NewYork, 1959).
6. Zhang, Y., Lucovsky, G. and Whitten, J. L., unpublished.
7. Tippins, H. H., J. Phys. Chem. Soilds **27**, 1069 (1966).
8. Cox, P. A., "Transition Metal Oxides" (Oxford Science Publications, Oxford, 1992), Chap. 2.
9. Rayner, Jr., G. B., Kang, D., Zhang, Y. and Lucovsky, G., J. Vac. Sci. Technol. **B 20**, 1748 (2002).